

# Features of $\mu$ -candidate events

Armando Lanaro (CERN)

March 18, 2002

## Abstract

We have studied reconstructed events for which at least one of the particles is a muon candidate. We investigate the origin of such muons (decay point of the parent pion, muons from target, halo muons), the pion contamination to the muon event sample, and the fraction of undetected muons in the pion event sample. Finally, we estimate the proton contamination in the sample of positively charged accidental particles.

## 1 Introduction

The analysis is based on a data sample consisting of about  $130 \times 10^6$  triggers (33 runs) collected during the summer of 2001, using a Ni target. Events were reconstructed using two software packages: the standard Ariane code (hereafter called **standard**) and an improved code which includes independent upstream tracking based on the combined information from MSGC and SFD hit patterns (hereafter called **standard+MSGC**). Reconstructed events were further selected by requiring:

- $Q_x, Q_y < 6 \text{ MeV}/c, Q_L < 45 \text{ MeV}/c$ ;
- presence of ADC amplitude in IH (single or double ionisation).
- presence of 2 hits in both x and y plane of SFD or 1 hit in one SFD plane matching a double ionisation signal in the corresponding strip of IH;

Events with  $e^+$  and/or  $e^-$  candidates were not rejected.

About 0.3% (435160 events) of the initial statistics survived the above selection criteria.

The identification of a  $\mu$ -candidate event is done during reconstruction using the algorithm extensively described in ref.1. According to such muon identification method the fraction of  $\mu$ -candidate events in the selected sample is  $\approx 10\%$ , for both correlated and accidental events, when reconstruction is done using the **standard** code. When using the **standard+MSGC** code this fraction becomes 9%. Muon events are largely (95%) events with only one charged muon (muonflag=1,2 according to ref.1), with an associated track coming from the target, i.e. participating to the vertex fit. In this analysis we assume that all muon candidates are

true muons, in the sense that we have no mean to distinguish between a real muon and a pion punching through the iron absorber placed in front of the muon detector. Previous investigations have concluded that the percentage of punch-through muons is however at the level of few percent.

If not otherwise stated, our results are based on information provided by the **standard** reconstruction method.

## 2 Event topology at target

In Fig. 1 the distribution of the  $x$  and  $y$  track coordinates at the target is shown for both the event samples without muons (Fig. 1a-c), and with muons (Fig. 1b-d). The distributions of events with muon candidates are wider with respect to those without muon candidates.

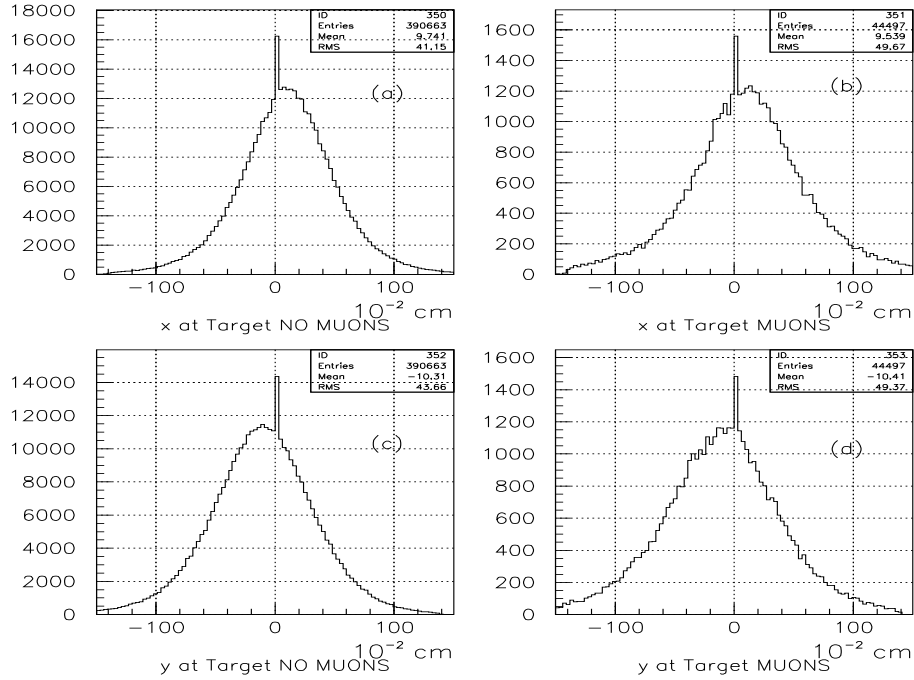


Figure 1: Distributions of track coordinates at target: (a)  $x$  no muon sample; (b)  $x$  muon sample; (c)  $y$  no muon sample; (d)  $y$  muon sample.

This can be seen also in Fig. 2, where the distribution of the relative distance in the  $xy$  plane between the extrapolated track coordinates at the target is shown. The fraction of  $\mu$ -candidate events increases when the relative distance is larger as shown in Fig. 2c. Indeed, the direction of reconstructed muons originating from pion decay upstream the DC will have a small kink with respect to the direction of the parent pion. Such small deflection will not prevent the event to

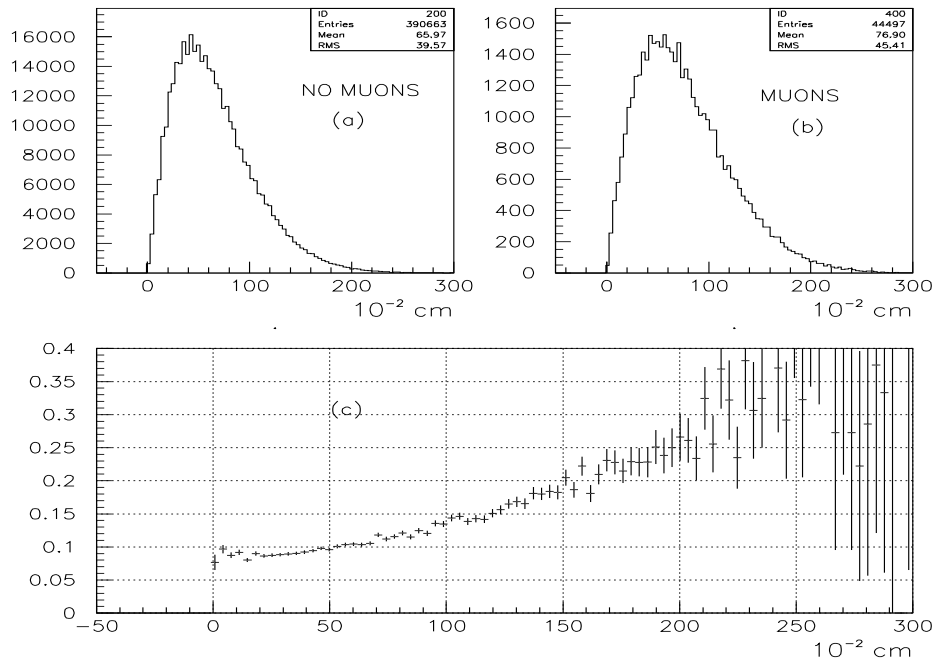


Figure 2: Distributions of relative distance of tracks at target for: (a) events without muon candidates; (b) events with muon candidates. (c) Ratio between distribution (b) and (a).

be reconstructed; it might lead, however, to larger values of the impact distance at the target. Muons from the proton beam halo or from pion not coming from the target might show similar features.

### 3 Sources of muons

Fig. 3 shows the ratio between the  $Q$  spectra of the event sample without muons and the overall data sample, that is, with and without muons, for correlated (Fig. 3a) and accidental (Fig. 3b) pairs. Whereas the distribution of Fig. 3b is flat, that of Fig. 3a indicates that the rejection of muon events leads to a relative excess yield of low- $Q$  ( $Q < 10$  MeV/ $c$ ) correlated events.

The analysis of  $Q_L$  spectra provides a mean to determine the origin of muons. Our analysis is based on the evidence that the yield of correlated pions with very small relative values of  $Q_L$  is dramatically increased by the Coulomb enhancement factor. This is clearly shown in Fig. 4a-b. Accidental pairs (Fig. 4c-d) show, on the contrary, no Coulomb correlation enhancement. The Coulomb peak is even more evident when a cut on  $Q_T$  is applied. Fig. 5a-b show the  $Q_L$  spectra of correlated pairs with  $Q_T < 2$  MeV/ $c$ . The  $Q_L$  distributions of correlated events with muons (Figs. 4b,5b) and events after muon rejection (Figs. 4a,5a), show different Coulomb peak

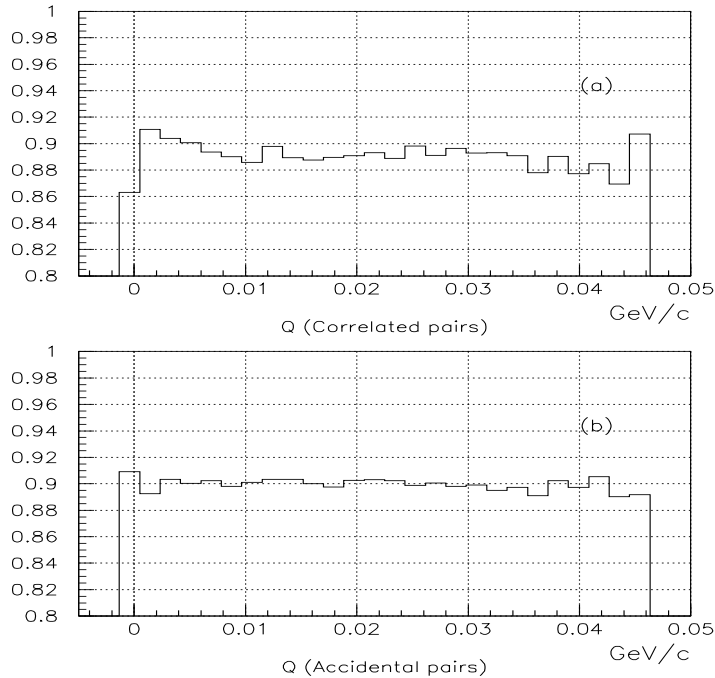


Figure 3: Ratio between the  $Q$  distribution of events without muons and that of events with muons. (a) Correlated pairs; (b) accidental pairs.

heights, in general higher for the latter. We have quantified such difference by measuring the ratio of peak over valley ( $P/V$ ), where peak is the height of Coulomb enhancement and valley is the height of the distribution outside the range  $|Q_L| < 15$  MeV/ $c$ .

We shall remark, however, that the majority of correlated particle pairs in the spectra of Figs. 4,5, are Coulomb pion pairs (pions from short-lived sources) and atomic pairs. In the present  $Q_L$  range the percentage of non-Coulomb pairs is small.

The ratio:

$$[(P/V) - 1]_{muons} / [(P/V) - 1]_{nomuons} \quad (1)$$

defines the probability that a  $\mu$ -event is linked to a Coulomb correlated  $\pi$ -event, that is, there is a muon coming from pion decay downstream the DC detector system, and the parent pion belongs to a Coulomb correlated pairs. If we define  $1 - \epsilon_{\pm}$  the probability for a Coulomb correlated  $\pi^{\pm}$  to decay after the DC into a detected  $\mu^{\pm}$ , then:

$$[(P/V) - 1]_{muons} / [(P/V) - 1]_{nomuons} = (1 - \epsilon_-) \times (1 - \epsilon_+) \quad (2)$$

Assuming  $\epsilon_- \approx \epsilon_+ = \epsilon$ , then from both Figs. 4a-b and Figs. 5a-b we obtain:

$$(1 - \epsilon)^2 = 0.68 \pm 0.02 \quad (3)$$

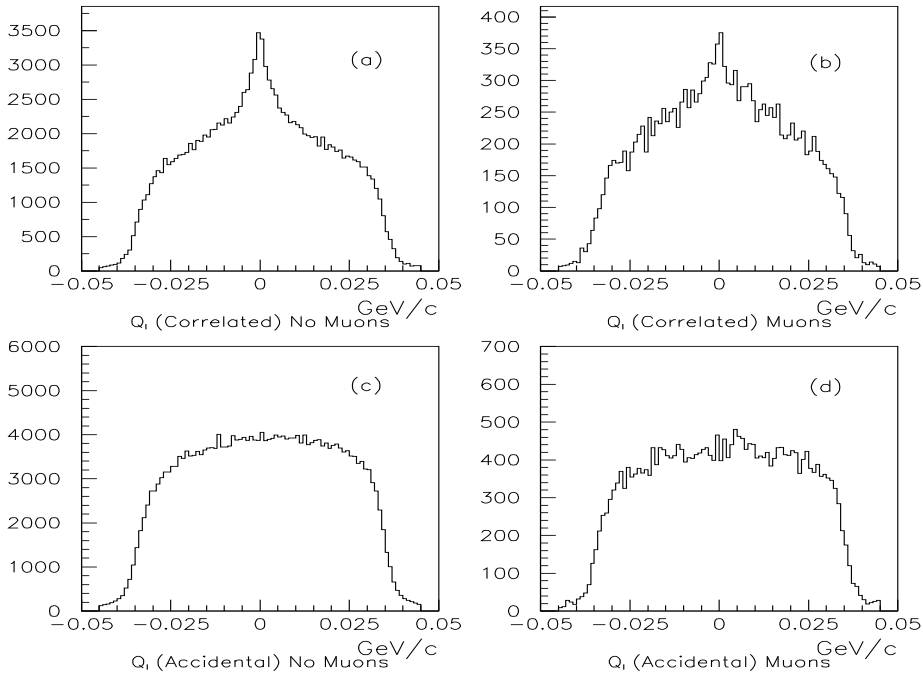


Figure 4:  $Q_L$  distribution for: (a) correlated events after muon rejection; (b) correlated muon events; (c) accidental events after muon rejection; (d) accidental muon events.

independent of the selected  $Q_T$  range. Therefore, about  $(1 - \epsilon) \simeq 82\%$  of the muons in the  $\mu$ -event sample come from pion decay downstream DC. The rest ( $\sim 18\%$ ) are muons originated from pions not coming from the target, or from non-Coulomb correlated pion pairs, or, finally, from straight muons from the target produced by short-lived sources (Coulomb correlated pion-muon pairs). (The latter is unlikely to occur because of the cut on  $|Q_L|$  imposed to the data. In fact, the  $\pi^\pm\mu^\mp$  Coulomb correlation peak would show at about  $Q_L \simeq \pm 45$  MeV/c, when the pion mass is assigned to the muon, thus at the edge of the  $Q_L$  spectrum.)

Since the fraction of  $\mu$ -events is about 10% of the total data sample, the  $\pi^\pm$  decay probability downstream DC in the full data sample is about 8%. This value compares well with the value predicted for a  $2\div 3$  GeV/c  $\pi^\pm$  decaying after 11m path length (distance between target and DC system). Given  $c\tau \simeq 7.8m$ , the calculated decay probability would be in fact  $9.4\div 6.3\%$ .

The fraction of muons associated to pions not coming from the target is about  $0.18 \times 0.10 = 2\%$  in the full data sample. This provides an estimate of the relative percentage of background particles in the selected data sample.

It is interesting to notice that the above conclusions do change once we repeat the analysis using the **standard+MSGC** reconstruction code. In this case, the fraction of  $\mu$ -events in the total sample is about 9%. Furthermore, the ratio in eq.1 is very close to unity, that is, all

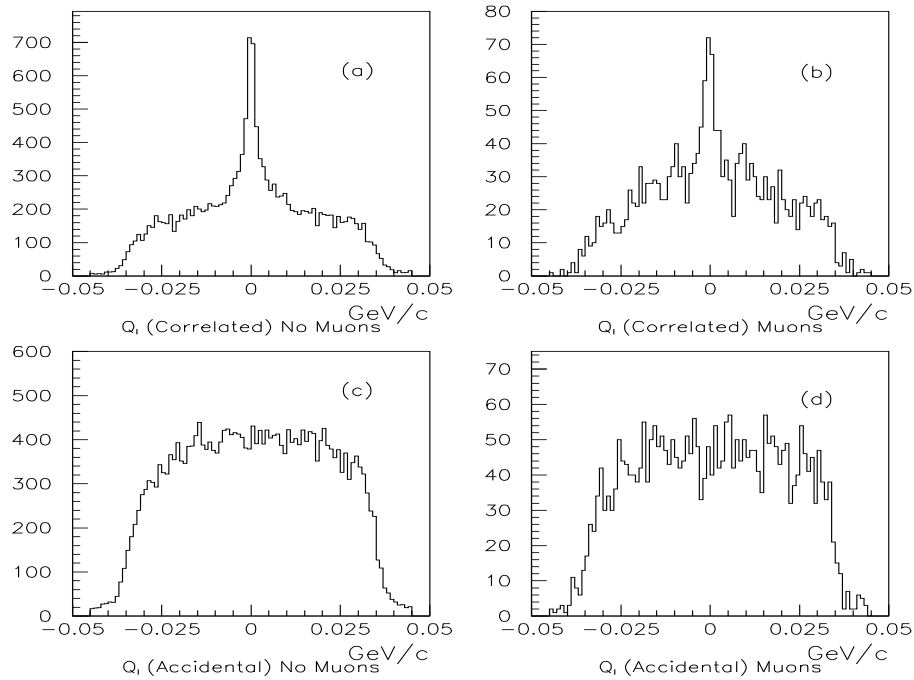


Figure 5: Same as Fig. 4 with an additional cut on  $Q_T < 2$  MeV/c.

detected muons are originated by Coulomb correlated pions decaying after DC. Therefore, the  $\pi^\pm$  decay probability downstream DC in the full data sample is about 9%, and the percentage of background particles (particles not coming from the target) is negligible.

All above estimates have a statistical uncertainty of the order of 10÷15%.

## 4 Effects of proton contamination

Proton misidentification in DIRAC leads to a distortion of the inclusive momentum spectra of positive pions with respect to the spectrum of negative pions. Protons in DIRAC have a rather harder momentum spectrum than  $\pi^+$ . For time-correlated particle pairs low-momentum protons are rejected by defining a sufficiently narrow time window around the peak of prompt pairs in the distribution of the time difference between positive and negative particles. An additional criteria on the maximum allowed value of the momentum of the positive particle ( $p_+ < 5$  GeV/c) allows to reject the fast proton contamination.

For accidental pairs, on the contrary, the proton contamination can only be estimated and taken into account on the basis of probabilistic arguments.

In Fig. 6 the momentum dependence of the ratio between the negative and positive particle yields is shown after rejection of the muon background. Fig. 6a shows the behaviour of corre-

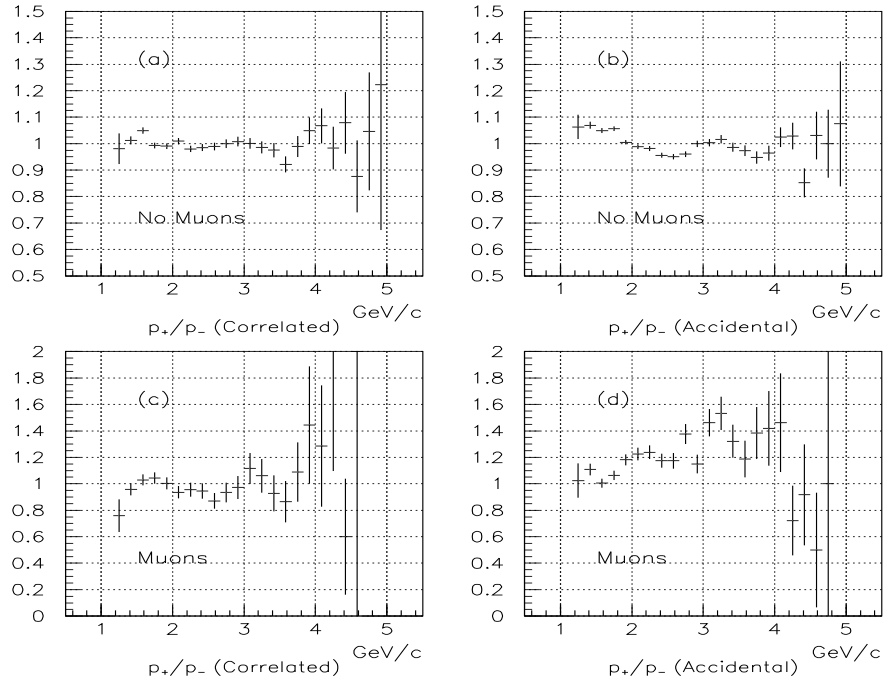


Figure 6: Momentum dependence of the ratio between negative and positive particles for: (a) correlated events after muon rejection; (b) accidental events after muon rejection; (c) correlated muon events; (d) accidental muon events.

lated events, whereas Fig. 6b is for accidental events. Because of the proton admixture to the accidental positive particles, the distribution of Fig. 6b shows clear deviations from unity. On the contrary, the distribution of Fig. 6a is rather flat over the entire momentum range.

The  $\mu$ -event sample is suitable for a different analysis of the proton contamination to the positive pion spectrum. Since the majority of muons originate from pion decay downstream the DC, and thus the reconstructed momenta are those of the parent pions, the proton contamination, larger at higher momenta, will affect the ratio between negative and positive muon yields. Because protons do not contribute to the  $\mu^+$  signal, the ratio  $\mu^-/\mu^+$  will increase when the momentum increases. This is clearly observed in Fig. 6d, which is obtained from the sample of accidental events.

For completeness, in Fig. 7 the momentum dependence of the ratio between the "tagged muon" and "muon free" yields is shown separately for positive (open circles) and negative particles (full circles). Fig. 7a refers to correlated events, whereas Fig. 7b is from accidental events. Proton contamination is responsible for the difference of the distributions of Fig. 7b.

From the relative excess of negative to positive muon events we have estimated the admixture of protons in the sample of accidental positive particles in the considered kinematical region.

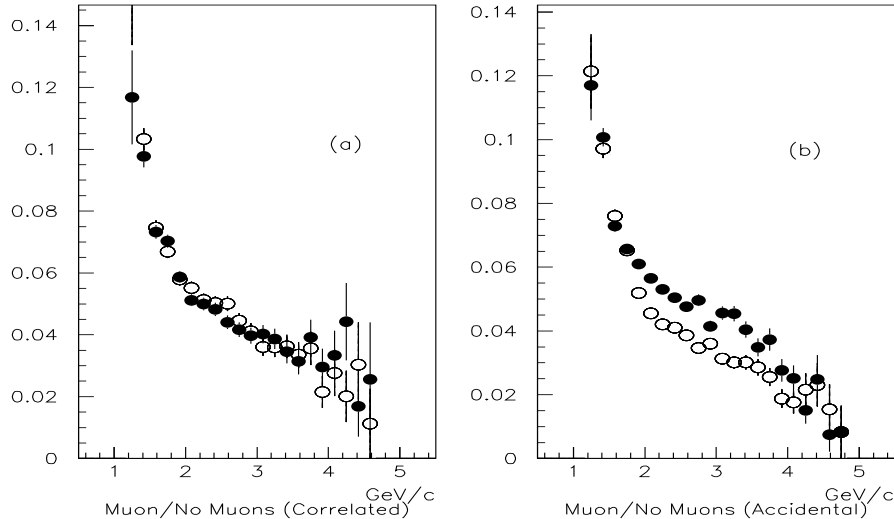


Figure 7: Momentum dependence of the ratio between muon and muon free events for positive (open circles) and negative (full circles) particles and for: (a) correlated and (b) accidental events.

We have defined the ratio:

$$\frac{N(p)}{N(\pi^+ + p)} = \frac{N(\mu^-) - N(\mu^+)}{N(\mu^-)} \times \frac{N(\pi^-)}{N(\pi^+)} \simeq 0.14 \quad (4)$$

where  $N(p)$  is the proton yield,  $N(\pi^\pm)$  are the yields of particles (mostly pions) after muon rejection and  $N(\mu^\pm)$  are the yields of  $\mu$ -tagged events.

An attempt to investigate the momentum dependence of the fraction of protons in the sample of muon-free accidental pairs (eq. 4) has led to the conclusion that the proton contamination increases from  $\sim 9\%$  at 1.4 GeV/c to  $\sim 30\%$  at 3.3 GeV/c.

## 5 Conclusion

Tagged muon events are mostly associated to the decay of pions downstream the DC system. When the parent pion comes from a correlated pair no information is lost concerning the production mechanism at the point of interaction. In particular, the evidence of Coulomb correlation in the final state is retained. In this respect, the fraction of tagged muon events could be included in the selected data sample for the search of atomic pairs. Nevertheless,



the topology of muon events at the production target is sometime peculiar and not well under control, due both to the fraction of background particles not coming from the target and to an undetectable fraction of muons originating at the target itself.

The sample of muon events provides, however, useful information on the effect of proton contamination to the positive particles when the latter are coming from accidental pairs. In this sense, such events are worth an independent analysis.

## References

- [1] V. Brekhovskikh and M.V. Gallas, *DIRAC Note 01-02* 14 March 2001.